Electrochemistry Communications 11 (2009) 1045–1047

Contents lists available at ScienceDirect

Electrochemistry Communications

journal homepage: www.elsevier.com/locate/elecom

InP as new anode material for lithium ion batteries

Yan-Hua Cui [a,b], Ming-Zhe Xue [a], Xiao-Lin Wang [b], Ke Hu [a], Zheng-Wen Fu [a,*]

[a] Shanghai Key Laboratory of Molecular Catalysis and Innovative Materials, Department of Chemistry, Fudan University, Handan Road 220, Shanghai 200433, China
[b] Institute of Electronic Engineering, China Academy of Engineering Physics, Sichuan 621900, China

ARTICLE INFO

Article history:
Received 21 February 2009
Received in revised form 9 March 2009
Accepted 12 March 2009
Available online 20 March 2009

Keywords:
InP
Lithium ion batteries
Pulsed laser deposition
Thin film
Anode

ABSTRACT

InP thin film has been successfully fabricated by pulsed laser deposition (PLD) and was investigated for its electrochemistry with lithium for the first time. InP thin film presented a large reversible discharge capacity around 620 mAh g^{-1}. The reversibility of the crystalline structure and electrochemical reaction of InP with lithium were revealed by using *ex situ* XRD and XPS measurements. The high reversible capacity and stable cycle of InP thin film electrode with low overpotential made it one of the promise energy storage materials for future rechargeable lithium batteries.

1. Introduction

Metal phosphides have been considered to be promise anode candidates for lithium ion batteries due to high reversibility and large capacities. Two kinds of metal phosphides were widely investigated [1–6]. Li–M–P as ternary lithium metal phosphides (M = Mn, Ti, V etc.), such as Li_7MnP_4, $Li_{5.5}Mn_{2.5}P_4$, Li_9TiP_4, Li_xVP_4 ($3 < x < 7.5$) with the intercalation/deintercalation of lithium exhibited larger specific capacities and flat voltage profiles in lithium ion batteries [1–3]. These performances should be related to a strong structural stability of the MP_4. Other binary metal phosphides (N–P with N = Co, Ni, Cu, etc.) show versatile electrochemical reaction mechanisms depending on the metal N. For example, a reversible conversion reaction of Li_3P into LiP was proposed for electrochemical reaction of CoP_3 with Li and the formed cobalt after the first discharging seem to be as an active spectator [4]. Gillot et al. suggested that the reversible reaction mechanism of NiP_2 with lithium was identified as a conversion reaction of NiP_2 into Ni and Li_3P [5]. Crosnier and Nazar reported a two-phase process of Cu_3P with Li in which copper is extruded from Cu_3P lattice with the formation of a metastable intermediate phase "$Li_xCu_{3-x}P$" ($x = 1$, 2, and 3) [6,7]. Apparently, the lithium electrochemical reaction of metal phosphides is still complicated and more work must be done to understand the nature of electrochemical reaction of metal phosphides with lithium.

InP is a semiconductor which has been widely used in high-power, high-frequency electronics and optoelectronics devices like laser diodes [8]. However, there was no available report on the electrochemical characterization of InP with lithium. In fact, indium-based alloy and compounds such as In–Sb, and In_2O_3 have been tested in lithium ion batteries for the improvements in battery performance [9–12].

In this paper, we firstly reported experimental results on the thin film fabrication of InP deposited by pulsed laser deposition (PLD). Its electrochemical and physical characterizations were examined by galvanostatic cycling, cyclic voltammetry (CV), X-ray diffraction (XRD) and X-ray photoelectron spectroscopy (XPS). The electrochemical reaction mechanism of InP with Li was discussed.

2. Experimental

The apparatus used for PLD has been described elsewhere [9]. The laser energy intensity was about 2 J cm^{-2}. Thin films were deposited on stainless steel substrate at 450 °C. The pressure of Ar ambient gas was controlled at 10 Pa. The targets were made from In and P powders (both 99.99%) with the molar ratios of 1:1.5 (In:P). An excessive P in a mixture target can compensate P loss due to its vacuum sublimation during laser ablation. XRD patterns of the thin films were characterized by a Bruker D8 advance diffractometer. XPS measurements were performed on a Perkin–Elmer PHI 5000C ECSA system and calibrated by using C 1s (284.6 eV) spectrum of hydrocarbon that remained in the XPS anal-

* Corresponding author. Tel.: +86 21 65642522; fax: +86 21 65102777.
E-mail address: zhengwen@sh163.net (Z.-W. Fu).

1388-2481/$ - see front matter © 2009 Published by Elsevier B.V.
doi:10.1016/j.elecom.2009.03.008

ysis chamber as a contaminant. The weight of thin film was examined by electrobalance (BP 211D, Sartorius).

For the electrochemical measurements, the cells were constructed by using the as-deposited InP thin film as working electrode and two lithium sheets as counter electrode and reference electrode, respectively. The electrolyte consisted of 1 M $LiPF_6$ in a non-aqueous solution of ethylene carbonate (EC) and dimethyl carbonate (DMC) with a volume ratio of 1:1. The cells were assembled in an Ar filled glove box. Galvanostatic cycling measurements were carried out at room temperature with a Land CT2001A battery test system. The cells were cycled between 0.01 and 3.0 V vs. Li^+/Li at a current density of 10 μA cm^{-2}. Cyclic voltammetry (CV) tests were performed with a scanning rate of 0.1 mV s^{-1} between 0.01 and 3.0 V on a CHI660A electrochemical working station (CHI Instruments, TN).

3. Results and discussion

Fig. 1a shows the discharge and charge curves of Li/InP cells. The initial open-circuit voltage potential of the cell was 2.8 V. The discharge plateaus in the galvanostatic curve can be attributed to the electrochemical behaviour of the as-deposited InP film electrode. The capacity of the first discharge is found to be around 780 mAh g^{-1}. The second discharge processes of the cell yield a reversible discharge capacity around 620 mAh g^{-1}, corresponding to 3.6 Li per InP. The subsequent charging curves are similar to the first. As shown in Fig. 1b, the capacity fade of the first cycle is about 20.5%, but the fade of 0.7% per cycle is obtained during 30 charge–discharge cycles, indicating good cycle performance. The ordinary In thin film prepared by pulsed laser ablation of In provide a reversible capacity of 396 mAh g^{-1}, corresponding to 1.7 Li per In with the larger fade.

Cyclic voltammogram (CV) curves of the as-deposited InP thin film were measured for the first three cycles and are shown in Fig. 2. In the negative sweep from 3.0 to 0.01 V, there are two relative large peaks at 0.22 and 0.01 V with three small peaks at 0.75, 0.57 and 0.48 V, respectively. These peaks could be related to the different reduction reaction processes of InP with Li. The corresponding oxidation peaks at 0.22, 0.42, 0.47, 0.65 and 0.80 V are observed in the positive sweep. In subsequent cycles, three main

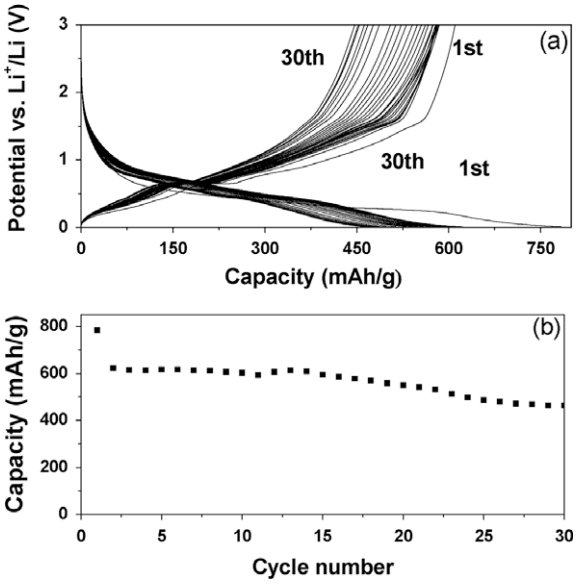

Fig. 1. (a) Charge–discharge cyclic curves and (b) the specific capacities as a function of cycle number for the as-deposited InP thin film at the current density of 10 μA cm^{-2}.

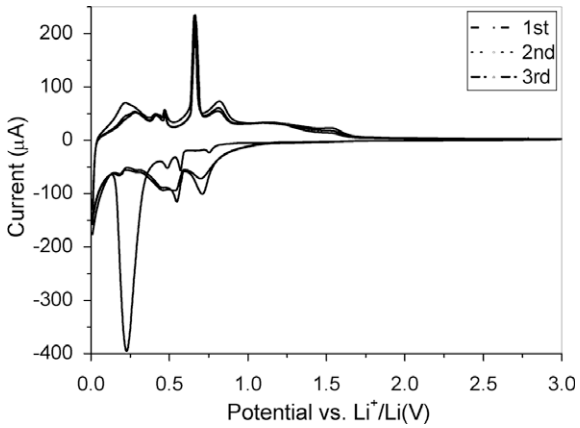

Fig. 2. First three CV profiles of InP thin film.

reduction peaks at 0.70, 0.53 and 0.01 V appear with the absence of strong peak at 0.22 V, while all oxidation peaks remain the same position. By comparing with both CV curves of the as-deposited InP thin film electrode and In [9], two main reduction peaks at 0.53 and 0.01 V and two oxidation peaks at around 0.42 and 0.65 V for both thin film electrodes indicate the formation of different In–Li alloys. One couple of cathodic and anodic peaks at 0.7 and 0.80 V for CV curves of InP thin film electrode could not be assigned to the oxidation and reduction of different In–Li alloys and Li_3P and should be attributed to the typical feature of InP.

XRD patterns obtained at different states of the first discharge and charge cycle are shown in Fig. 3. The XRD pattern of the as-deposited thin film was included for comparison (Fig. 3a), in which the diffraction peaks at 26.3° and 30.5° could be assigned to the (1 1 1) and (2 0 0) reflection of the cubic structure of InP (JCPDS card no. 73-1983), and another diffraction peak at $2\theta = 43.6°$ correspond to the SS substrate (marked by asterisk) and is overlapped with (2 2 0) reflection of the cubic structure of InP. It supports that the as-deposited thin film consists mainly of InP. After discharging to 0.01 V, these diffraction peaks from InP disappear (Fig. 3b) and some new peaks at 22.6°, 32.9°, 37.4° an 39.1° are observed and can be attributed to the diffraction peak of InLi(1 1 1), In(1 0 1), InLi(2 2 0) and In(1 1 0) (JCPDS cards no. 65-3019, and 85-1409), indicating that lithium reacts with InP thin film to form new In–Li alloy and parts of unalloyed In. No other diffraction peaks from Li_3P were detected. This may be due to the sizes of formed Li_3P par-

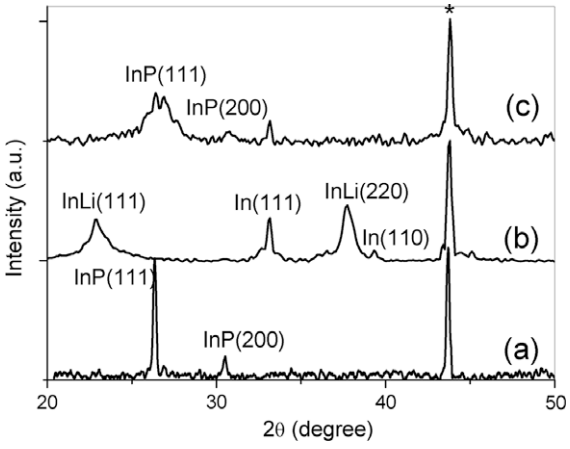

Fig. 3. *Ex situ* XRD pattern of InP thin film at various states during the first cycles of Li/InP cell with a limited voltage range of 0.01–3.0 V. (a) As-deposited; (b) discharging to 0.01 V; (c) charging to 3.0 V.

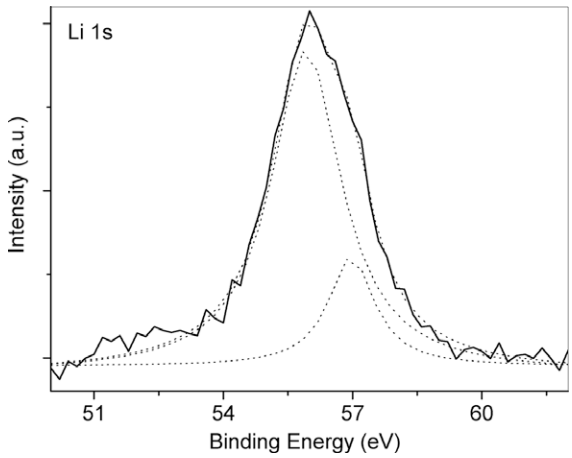

Fig. 4. Li 1s spectrum of InP thin film after discharging to 0.01 V.

ticles less than X-ray coherence length (6 nm), which could not be identified by XRD techniques. But Li_3P can be confirmed by Li 1s spectrum of thin film electrodes in the first cycle shown in Fig. 4. The measured solid curve in Fig. 4 could be deconvoluted into two components peaked at 55.9 and 56.9 eV with energy separation of 1.0 eV. According to previous studies [4,13], they can be attributed to Li binding energy for $LiPF_6$ (the residual electrolyte) and Li_3P, respectively. The electron binding energy of Li 1s peak at 56.9 eV indicates the formation of Li_3P during discharging reaction of InP with Li to 0.01 V.

When the cell is charged to 3.0 V, XRD patterns from InP appear with the existence of a small quantity of metal In as shown in Fig. 3c. This means that Li^+ is extruded from Li–In alloy and InP can be reversibly formed. It should be noted that the shape of InP(1 1 1) and (2 0 0) diffraction peaks after charging to 3.0 V become wider than that of the as-deposited thin film, indicating the decrease of crystalline size of electrochemically formed InP. According to Scherrer's formula, the crystallite size of reconstructed InP is reduced to 10 nm.

Based on the *ex situ* XRD and XPS results, the electrochemical reaction mechanism of InP with lithium might be expressed as follows,

$$\mathrm{InP} + (4-x)\mathrm{Li}^+ + (4-x)\mathrm{e} \rightarrow \mathrm{Li_3P} + (\mathrm{LiIn})x + (1-x)\mathrm{In} \quad (1)$$

$$\mathrm{Li_3P} + \mathrm{LiIn} \leftrightarrow \mathrm{InP(nanosized)} + 4\mathrm{Li}^+ + 4\mathrm{e}. \quad (2)$$

The irreversible reaction (1) occurs in the first discharging process with the structure transformation of initial poly-crystalline InP into the nanosized LiIn and Li_3P. Reaction (2) happens in subsequent cycles and includes two step reactions. The first step is fully reversible alloying/dealloying reaction of In. The second step involves in the phosphorization/reduction reaction of In. The existence of part of metal In in the charged film (Fig. 3c) indicates that In could not fully converse to InP. This reaction mechanism can explain the high reversible capacity of 620 mAh g^{-1} (corresponding to 3.6 Li per InP) in the galvanostatic cycling more than the maximum capacity of Li-alloying with indium (LiIn, corresponding to 1 Li per InP). These steps are in accord with CV curves (Fig. 2). Two couple of reduction peaks at 0.53 and 0.01 V and oxidation peaks at around 0.42 V and 0.65 V could be assigned to alloy–dealloy reaction, and one couple of cathodic and anodic peaks at 0.70 and 0.80 V could be attributed to the phosphorization/reduction reaction of In. Apparently, In can drive the decomposition of Li_3P with the formation of nanosized InP. Interestingly, the crystalline InP thin film can fully reversibly decompose and form as confirmed by XRD. In other words, the electrochemical reaction of nano-sized metal In with Li_3P formed after the initial discharge process can produce the crystalline InP when the cell is charged. It is utterly different from lithium electrochemistry of zinc phosphides, in which the reconstruction of starting material was not observed [14,15]. In addition, it can be found that the Li/InP cells has less polarization determining by the potential difference between the charging potential and discharging potential if comparing other metal phosphides or metal oxides reported previous [4–8,11,12].

4. Conclusions

A novel anode material of InP thin film prepared by PLD for lithium ion batteries was firstly reported. Our results suggested that nanostructured thin film electrode of InP exhibited high reversible capacity around 620 mAh g^{-1} with low potential, corresponding to 3.6 Li per InP. By using *ex situ* XRD and XPS measurements, a reversible crystalline structure and electrochemical reaction mechanism of InP with lithium was revealed. Our results demonstrated the potential of InP thin film electrode as storage energy materials for future rechargeable lithium batteries.

Acknowledgements

This work was financially supported by the Science and Technology Foundation of China Academy of Engineering Physics (2007A05002), Science and Technology Commission of Shanghai Municipality (08DZ2270500), the NSFC (Project No. 20773031), the "973" Projects (2007CB209702) and "863" Projects (2007AA03Z322).

References

[1] F. Gillot, L. Monconduit, M.L. Doublet, Chem. Mater. 17 (2005) 5817.
[2] M.P. Bichatt, F. Gillot, L. Monconduit, F. Favier, M. Morcrette, F. Lemoigno, M.L. Doublet, Chem. Mater. 16 (2004) 1002.
[3] M.L. Doublet, F. Lemoigno, F. Gillot, M.L. Doublet, Chem. Mater. 14 (2002) 4126.
[4] V. Pralong, D.C.S. Souza, K.T. Leung, L.F. Nazar, Electrochem. Commun. 4 (2002) 516.
[5] F. Gillot, S. Boyanov, L. Dupont, M.L. Doublet, M. Morcrette, L. Monconduit, J.M. Tarascon, Chem. Mater. 17 (2005) 6327.
[6] O. Crosnier, L.F. Nazar, Electrochem. Solid-State Lett. 7 (2004) A187.
[7] M.P. Bichatt, T. Politova, J. Pascal, F. Favier, L. Monconduit, J. Electrochem. Soc. 151 (2004) A2074.
[8] B.L. Welss, Properties of Indium Phosphide, Institution of Electrical Engineers, 1991.
[9] J.T. Vaughey, J.O. O'Hara, M.M. Thackeray, Electrochem. Solid-State Lett. 3 (2000) 13.
[10] K.C. Hewitt, L.Y. Beaulieu, J.R. Dahn, J. Electrochem. Soc. 148 (2001) A402.
[11] T. Sarakonsri, C.S. Johnson, S.A. Hackney, M.M. Thackeray, J. Power Sources 153 (2006) 319.
[12] Y.N. Zhou, H. Zhang, M.Z. Xue, C.L. Wu, X.J. Wu, Z.W. Fu, J. Power Sources 162 (2006) 1373.
[13] J. Chastain (Ed.), Handbook of X-ray Photoelectron Spectroscopy, Perkin–Elmer Corporation, Eden Prairie, 1992.
[14] M.V.V.M. Satya Kishore, U.V. Varadaraju, J. Power Sources 144 (2005) 204.
[15] M.P. Bichat, L. Monconduit, J.L. Pascal, F. Favier, Ionics 11 (2005) 66.